04

Synthesis of hafnium carbide powder in atmospheric arc plasma

© Yu.Z. Vassilyeva, P.V. Povalyaev, A.P. Korchagina, S.A. Yankovsky, A.Ya. Pak

Tomsk Polytechnic University,
Tomsk, Russia
e-mail: yzv1@tpu.ru

Received November 9, 2022
Revised April 10, 2023
Accepted April 12, 2023

The paper presents a method, implemented for the first time, for the thermal synthesis of hafnium carbide powder using a DC arc discharge initiated in the open-air atmosphere. Based on the results of the series of experiments, the dependences of the current strength of the power source and the time of thermal treatment on the phase composition of the resulting powder product were established. Required parameters have been determined to ensure the synthesis of a powder containing ~ 98 mass.% of the cubic phase of hafnium carbide: heat treatment of the initial mixture containing the stoichiometric ratio of hafnium to carbon for 60 s at a current of 220 A. The size, shape, and substructure of particles of the synthesized carbide are characterized. The differential thermal analysis carried out in an oxidizing medium showed that the obtained hafnium carbide powder is oxidized most intensively at a temperature of $\sim 700^{\circ}$C.

Keywords: hafnium carbide, atmospheric plasma, electric arc reactor, self-shielding environment.

DOI: 10.21883/0000000000

Introduction

With the aerospace industry development the need for materials that can withstand high temperatures and have unique physical properties is growing every year. The most promising compounds suitable for these purposes are transition metal carbides, which form a family of ultra-high temperature ceramics (UHTCs) [1–3]. One of the compounds included in this family and attracting considerable attention due to its physicochemical properties is hafnium carbide (HfC). Ultra-high melting point ($> 3800^{\circ}$C) [4–8], high modulus of elasticity (350−510 GPa) [9,10] and hardness (26.1 GPa) [11,12], excellent corrosion resistance [13,14] and thermal shock resistance [9], good chemical stability [15–18] and low electrical resistivity [12,14] make this material promising for use in various industries. Hafnium carbide can be used to produce cutting tools [19–21], thermal field emission sources [2,19,21], hypersonic aircrafts [5,12] and other products operating in extreme conditions [22]. There are several ways to obtain hafnium carbide: the process of spark plasma sintering (SPS) [3,14,20], high-energy mechanical grinding of powder mixtures containing metal and carbon, followed by annealing in an inert atmosphere [23], carbothermal reduction of metal oxides [19,21,22], direct metal carbidization [24] and other methods. In cases where HfC coatings are required, chemical vapor deposition (CVD) processes are used [10,16,25]. Despite the numerous different methods of synthesis, each of them has certain disadvantages, and, because of this, it is advisable to develop simple and energy-efficient methods for obtaining hafnium carbide.

A well-known method for obtaining various ceramic materials is the electric arc method. The necessary high temperature for material synthesis is provided by the arc discharge plasma in the reaction zone. In the previous papers of the authors of this paper, a non-vacuum electric arc method for the synthesis of silicon and tungsten carbides was described and tested [26,27]. The synthesis process was carried out in an open air environment, which became possible due to the effect of self-shielding of the reaction zone by gases of carbon monoxide and carbon dioxide [27]. Usually, electric arc synthesis is carried out in the inert gas atmosphere, which subsequently affects the cost of the final product due to cost of additional equipment (vacuum pump, sealed chamber etc.) [28–30]. Since the described method does not require the creation of the inert medium, this makes it possible to significantly simplify the design of the arc reactor.

The aim of this paper is to develop an original approach to obtaining the powdered hafnium carbide by thermal synthesis using the direct current arc discharge initiated in the open air environment and to study the obtained product by X-ray diffractometry, scanning electron microscopy, and transmission electron microscopy.

1. Materials and methods

1.1. Initial materials

Hafnium powders (manufacturer Shenzhen Finida Imp& Exp Co., Ltd, average particle size10−5 μm, purity 99.9%) and carbon of grade „Sibunit“ (manufacturer Federal State Budgetary Institution Institute of Problems of Hydrocarbon

Processing, SB RAS, mesoporous structure, specific surface area 355 m^2/g, ash content is maximum 1.0%).

The stoichiometric mixture was prepared according to reaction (1) by weighing the exact amount of the individual components and mixing in a Mixer/Mill 8000M vibrating ball mill for 30 min in a silicon nitride vessel Si_3N_4:

$$Hf + C \rightarrow HfC. \quad (1)$$

1.2. Laboratory arc reactor

The electric arc reactor used for the synthesis of hafnium carbide is a combined type reactor, the simplified diagram of which is shown in Fig. 1.

The reactor consists of direct current source *1* with operating current range 20–220 A, connected to a standard electrical network 220 V, and automated drive for moving the anode to control the discharge gap, where current-carrying electrode holders *2* are installed. With this modification of the discharge circuit the graphite crucibles of different sizes are used (hereinafter, the small crucible *3* and the larger crucible *4*). The small crucible is used to charge the initial mixture *5*. The contacts of the direct current source are connected to the current-carrying parts of the reactor: the negative terminal of the source is connected to the aluminum substrate for the crucibles, thereby the assembled crucibles act as a cathode, and the positive terminal of the source is connected to the electrode holder. In this system, the anode is a graphite rod *6*. When the anode comes into contact with the crucible, a short circuit occurs in the system, and when it is removed from the cathode, the electric arc discharge *7* is formed. Oxidation of the synthesis products is prevented by self-shielding of the reaction zone inside the larger crucible with CO and CO_2 gases, which was described both by the authors of other papers when obtaining carbon nanostructures [31], and in previous papers of the authors of this paper when obtaining silicon and tungsten carbides [26,27]. The oscilloscope *8* is present in the device circuit to record the electrical parameters of the system.

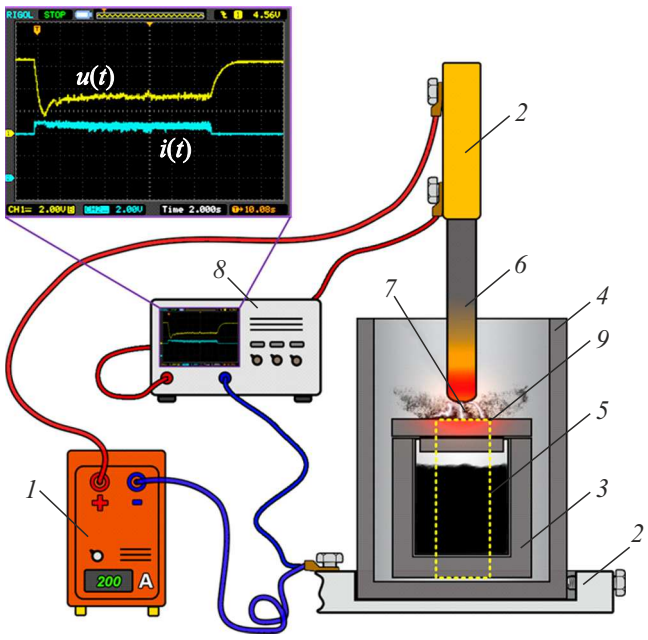

Figure 1. A simplified diagram of the electric arc reactor for producing hafnium carbide: *1* — DC source, *2* — current-carrying holders, *3* — small graphite crucible, *4* — large graphite crucible (cathode), *5* — initial mixture, *6* — graphite rod (anode), *7* — electric arc discharge, *8* — oscilloscope, *9* — groove in large graphite crucible (for thermal imaging; groove is made only if visual recording system is used).

1.3. Experiment

In the course of the study two series of experiments were carried out (excluding pre-commissioning): in the first series, the current strength was increased from 50 to 220 A under thermal exposure to electric arc plasma for 60 s, in the second series the duration of exposure was changed from 15 to 75 s with 15 s step.

A small graphite crucible with an inner diameter of 14 mm was filled with a sample having weight ≈ 1.5 g (the outer dimensions of the crucible were: diameter 20 mm and height 20 mm). To avoid the reaction between the graphite crucible and the powder, an interlayer of graphite sheet 0.2 mm thick was placed [32]. The small graphite crucible was closed with a lid and placed in a larger graphite crucible (external diameter 30 mm and height 40 mm). Between the two crucibles a graphite sheet 0.5 mm thick is installed to prevent the small crucible from moving inside the large crucible. The crucibles with powder were placed on the aluminum substrate of the laboratory electric arc reactor, which served as a current-carrying part, after which small graphite crucible was exposed to the electric arc discharge by bringing the graphite rod (length 100 mm and diameter 8 mm) to it using the automated electric drive.

Fig. 1 (enlargement of the oscilloscope screen) shows typical voltage and current oscillograms recorded during the thermal treatment of the feedstock with electric arc plasma. At the initial moment of time, the arc voltage is equal to the open-circuit voltage of the DC source and is 65 V, the current does not flow in the discharge circuit. Further, at the moment of the arc discharge initiation by contacting the anode with the lid of the small graphite crucible, current begins to flow in the discharge circuit, the voltage decreases to the minimum value (~ 15 V) — short circuit voltage. After the discharge gap is established, the voltage and current stabilize to the level of the arc stage (depending on the exact experiment ~ 30–35 V). Then, after the end of the thermal effect of the DC arc discharge, the discharge circuit is opened by removing the anode from the cathode, as a result the arc discharge is extinguished, and the voltage on the electrodes is restored to the open circuit voltage. By multiplying the arrays of current and voltage, the dependence of the electric power change versus time was obtained, followed by its integration over time the amount of energy supplied to the system was calculated.

Table 1. Estimation of energy parameters in series of experiments

№	I, A	t, s	W, kJ
1	220	75	336
2	220	60	281
3	220	45	213
4	220	30	173
5	220	15	73
6	220	60	281
7	150	60	258
8	100	60	194
9	50	60	98

Table 1 presents the results of estimating the energy parameters of the series of experiments performed (discharge circuit current I, duration of the heat treatment t, amount of supplied energy W).

To study the temperature field during the thermal impact of DC arc discharge, the thermal imaging was performed using Optris PI 1M infrared camera at current of the discharge circuit 220 A. To do this, a groove *9* in the shape of a rectangle was made in the wall of the larger crucible (Fig. 1), equal to the height of the small crucible; the arc plasma region was separated from the camera lens by a protective screen to exclude the possibility of the camera matrix damage by arc radiation. The temperature in the upper and lower parts of the small crucible filled with the initial mixture was measured, and the integral value over the region was calculated (in a standardized infrared camera software package). As can be seen in Fig. 2, there is a temperature gradient along the crucible on the outer wall of the small crucible, the magnitude of which decreases with increasing duration of thermal exposure. According to diagram of states hafnium-carbon [33], for receiving hafnium carbide HfC temperature from ~ 1900 to $\sim 2300^\circ$C (from ~ 2173 to ~ 2573 K) are needed. Papers are known, in which hafnium carbide was received at temperatures 1500–1600°C by method of pyrolysis of [12,18,34], 1600–2100°C by SPS [6,14], 1200–1600°C by CVD method [15,16], and also at temperature 1075°C by CVD method [35] and at 750°C by annealing after grinding in mill [23]. According to the obtained thermograms (Fig. 2), for the duration of exposure 30–60 s, the average value of the temperature of the outer wall of the small crucible is about 1250–1350°C, and the maximum temperature exceeds 1700°C, therefore, the realized conditions are sufficient to obtain hafnium carbide by this method. Besides, the groove made for imaging in the larger crucible obviously increases the loss of thermal energy in the system, so the data obtained are somewhat underestimated relative to the actual synthesis process.

1.4. Analysis of obtained results

synthesized samples studied by various methods , including method of X-ray diffraction analysis on diffractometer Shimadzu XRD-7000S ($\lambda = 1.54060$ Å), by scanning electron microscopy on microscope Tescan Vega 3 SBU with attachment for energy dispersive analysis (EDA) Oxford X-Max 50, by method of transmission electron microscopy on microscope JEOL JEM 2100F, by method of differential thermal analysis on device Netzsch STA 449 F3 Jupiter (Netzsch, Germany).

2. Results and discussion

Fig. 3 shows X-ray diffraction patterns of samples obtained at current strength of 220 A and different processing times of the initial mixture 15–75 s (Fig. 3, *a*); at exposure for 60 s and different current strength 50–220 A (Fig. 3, b). The main phase in all samples is the hafnium carbide phase (the closest model in the database: ICDD #00-039-1491), which confirms the successful synthesis of the desired product by the method of electrothermal exposure to atmospheric plasma. However, as can be seen from Fig. 3, at the minimum arc discharge duration (15 s), as well as at the minimum current strength (50 A), the X-ray patterns contain diffraction peaks of the initial hafnium (ICDD #00-038-1478) and traces of hafnium oxide (ICDD #00-034-0104). This can be explained as follows. As noted earlier, in the process of synthesis the self-shielding medium consisting of CO and CO_2 gases is formed in the cavity of the graphite crucible, which protects the reaction zone from the ingress of atmospheric oxygen and, accordingly, from the synthesis products oxidation. Probably, at 15 s, the shielding medium is formed in amount that does not completely cover the reaction zone, as a result of which an insignificant amount of hafnium oxide is formed in the product. At current strength of 50 A, the heating temperatures of the feedstock are minimal in comparison with other conditions under consideration, therefore, there is insufficiently intense carbon sputtering from the electrode surface during their combustion to form the protective atmosphere, therefore, more intense maxima of hafnium oxide are observed on the X-ray diffraction pattern. In both cases, insufficient energy parameters determine the presence of unreacted initial hafnium in the powders. As can be seen, further, with increase in both the arc exposure time and the current strength, the diffraction maxima of hafnium oxide disappear. Therefore, the higher the current strength and the longer the plasma exposure time are, the larger the shielding zone is. It was established that at current strength > 100 A and plasma treatment time > 30 s the sufficient volume of shielding gases — carbon monoxide and carbon dioxide — is formed to shield the reaction zone at the considered parameters of the discharge circuit. However, on the diffraction patterns of samples synthesized at 30 and 45 s (Fig. 3, *a*), as well as samples obtained at 100 A (Fig. 3, *b*), maxima were identified that belong to the initial hafnium phase. This may

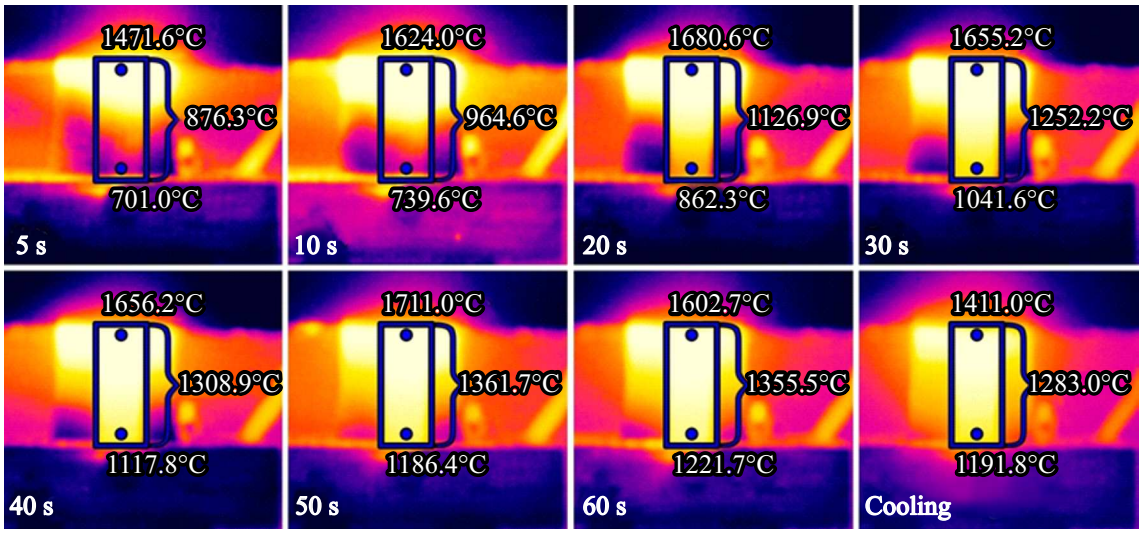

Figure 2. Distribution of temperature field during the thermal effect of direct current arc discharge.

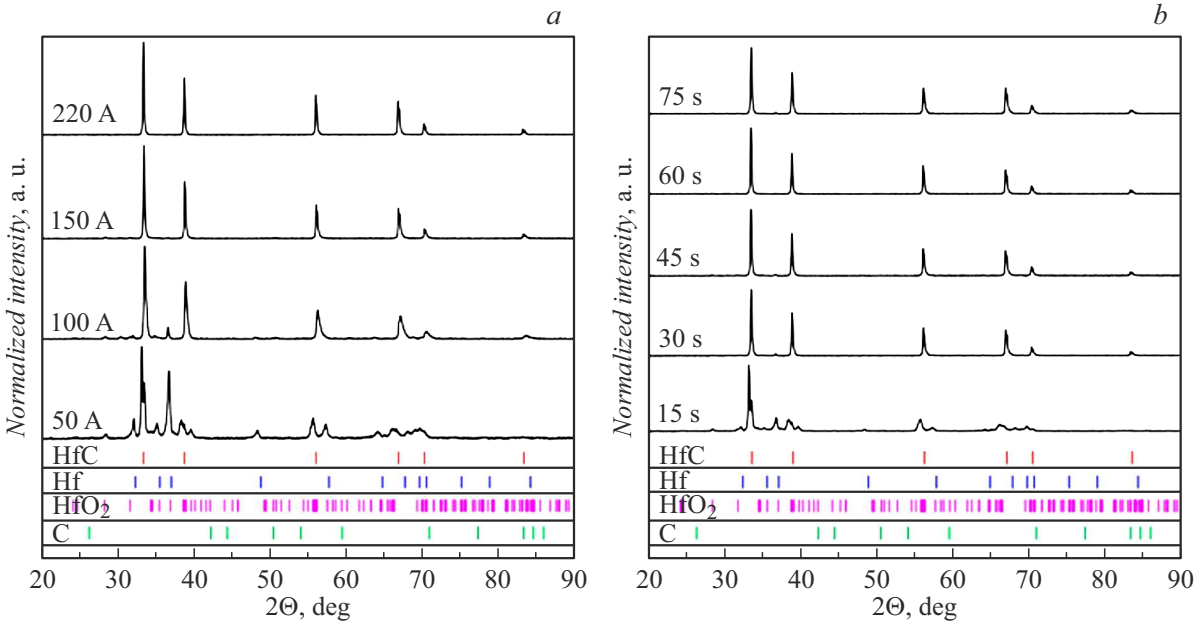

Figure 3. X-ray diffraction patterns of samples obtained at different durations of thermal exposure to electric arc plasma 15–75 s (*a*) and different current strengths 50–220 A (*b*).

indicate that the amount of energy supplied is not sufficient for the complete processing of the feedstock into carbide. It is determined that with increase in the time of the electric arc exposure, the amount of supplied energy increases from ~ 73 to ~ 336 kJ, while with increase in the current strength, the energy varies from ~ 98 to ~ 281 kJ (Table 1). The X-ray diffraction patterns of the samples obtained under the thermal action of the electric arc plasma for 60 and 75 s do not differ significantly. Therefore, we can conclude that processing the initial mixture containing the stoichiometric ratio of hafnium to carbon for 60 s at current strength of 220 A is sufficient for the synthesis of hafnium carbide. In this case, the specific amount of energy is ~ 295 kJ/g (according to the mass of the initial mixture). For samples obtained under certain conditions (60 s, 220 A), the lattice parameter was measured (within the accuracy of the used X-ray diffractometer and the actual possibilities of ensuring accuracy based on the results of goniometer calibration), the value of which was 4.634 ± 0.003 Å. This value corresponds to the fraction of carbon from ~ 45 to ~ 47 at.% [33], which may mean that, in addition to the electrode material, carbon is also consumed from the stoichiometric mixture of hafnium and carbon powders to form an autonomous gaseous medium. At the same time, it is known that

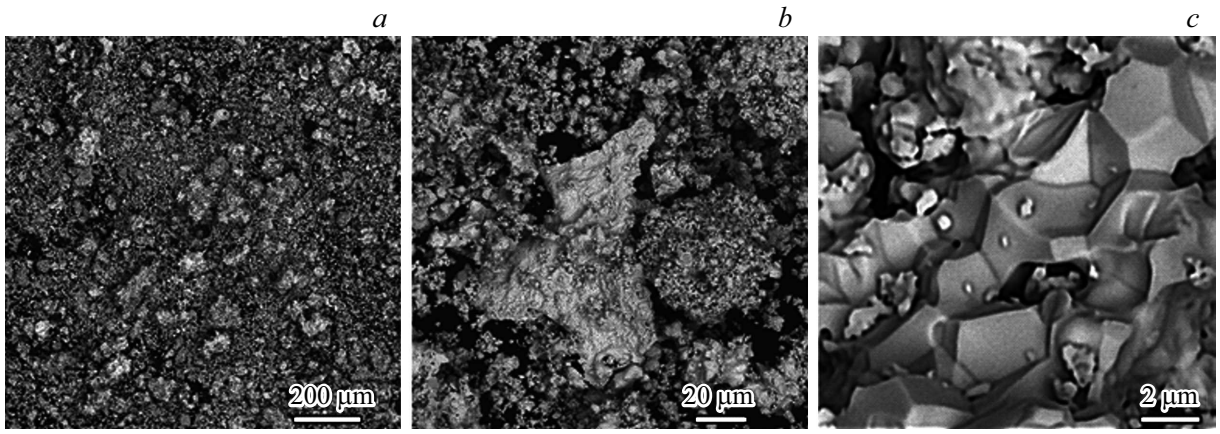

Figure 4. SEM image of sample obtained at 220 A, 60 s: *a* — overview image; *b, c* — particle images.

oxygen can also affect the lattice parameter, forming a solid solution, overestimating the lattice parameter, as shown by other researchers, for example, when studying the processes of zirconium carbide formation in CO [36] atmosphere. Thus, the issue of determining the exact C/Hf ratio, as well as studying the possibilities of controlled synthesis of nonstoichiometric compounds, is quite complex and little studied, in particular, within the electric arc method used.

For the powder synthesized at current strength of 220 A and a duration of thermal treatment with atmospheric electric arc plasma of 60 s, a series of analyzes was carried out, in particular, the morphology of the micron fraction of the synthesized product was studied by scanning electron microscopy. To increase the electrical conductivity of the sample, a layer of carbon was deposited on its surface. SEM images were obtained in the back-scattered electron mode. It can be seen from the overview image (Fig. 4, *a*) that the particles in the sample are evenly distributed: most of them are represented by flaky particles of size$\sim 1-5\,\mu$m [12,22,37], there are also larger elongated particles (longitudinal size $\sim 90\,\mu$m, transverse — $\sim 55\,\mu$m) and particle agglomerates. The sizes of clusters of agglomerates range from ~ 50 to $\sim 200\,\mu$m. Besides, on some SEM images it is possible to identify particles with hexagonal faces, the size of the hexagonal face is $\sim 4\,\mu$m; similar particles are encountered in the synthesis of hafnium carbide by other methods in a number of papers [38,39].

According to the EMF, the main chemical elements in the composition are hafnium and carbon, quantitative data are not given due to the known errors of the EMF method for light elements and the carbon layer deposition during sample preparation. Besides, an insignificant amount of impurities in the form of copper, aluminum and iron atoms with a total content of maximum 2 at.% was recorded. The presence of impurities can be due to the ingress of atoms from the current-carrying parts of the electric arc reactor during the arc discharge combustion.

Transmission electron microscopy was used to obtain bright-field images of the nanosized fraction of the sample synthesized by the electrothermal method, as well as the corresponding electron diffraction patterns (Fig. 5, *a, b*). Based on the data obtained, it can be concluded that the sample contains both polycrystalline structures and individual single crystals. Note that based on the identified reflections on the electron diffraction patterns (Table 2), there is an oxide film on the surface of the particles, consisting of HfO_2. The formation of oxide film can occur due to certain conditions of storage, transportation, or cooling of both the initial and synthesized powders without protective atmosphere in air, as well as during the sample preparation for study. Since the TEM method is local, and there are no oxide diffraction maxima on the X-ray diffraction pattern of the studied sample (Fig. 3), it can be stated that the amount of oxygen in the sample is minimal, below the sensitivity limit of the X-ray diffractometry method. The comparison of interplanar spacings presented in Table 2, identified from electron diffraction patterns (Fig. 5, *a, b*, insert), allows us to conclude that the polycrystal contains hafnium carbide and may contain phases of hafnium, carbon in the form of graphite, and hafnium oxide.

The value of interplanar spacings determined from high-resolution TEM images (Fig. 5, *c*) $d \sim 0.234$ and ~ 0.231 nm within the error corresponds to the analogous value of the standard hafnium carbide $d_{(200)} = 0.2319$ nm. Differences in the values of interplanar spacings may indicate distortions of the crystal lattice due to the possible presence of impurities in the lattice [40], as noted earlier, as well as by carbon vacancies.

The study of the oxidation processes of hafnium carbide sample synthesized at current strength of 220 A and a duration of thermal treatment by atmospheric electric arc plasma of 60 s was carried out using a Netzsch STA 449 F3 Jupiter differential thermal analyzer. The sample 20 mg was distributed evenly over the bottom of the crucible and placed in a flow of oxidizing medium (air). The weighed portion with the sample was heated in a corundum crucible with a perforated lid to the temperature of 1000°C in order to completely oxidize it. The heating rate was

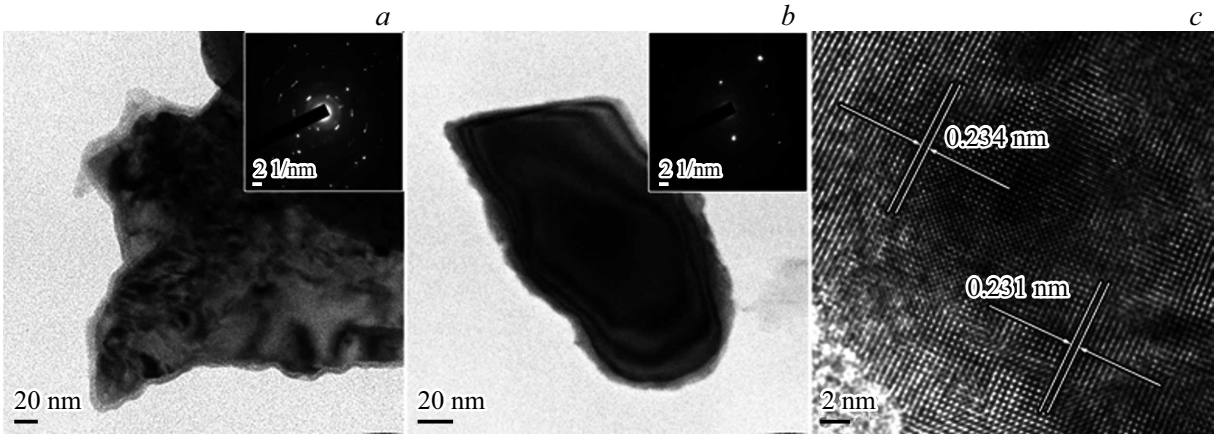

Figure 5. The results of transmission electron microscopy of powder obtained at 220 A, 60 s: *a* — TEM image, *b* — pattern of electron diffraction on selected area, *c* — high-resolution TEM image.

Table 2. Comparison of interplanar spacing data

SAED (fig. 5, *a*)	SAED (fig. 5, *b*)	PDF 4+			
d, Å		HfC (ICDD № 00-039-1491)	Hf (ICDD № 00-038-1478)	C (ICDD № 04-015-2407)	HfO_2 (ICDD № 00-034-0104)
3.00 ± 0.08				3.39 d_{002}	
2.74 ± 0.04		2.67 d_{111}	2.76 d_{100}		
2.41 ± 0.05	2.41 ± 0.01		2.42 d_{101}		2.43 d_{102}
1.68 ± 0.02				1.69 d_{004}	1.68 d_{202}
1.41 ± 0.04	1.44 ± 0.01	1.39 d_{311}	1.43 d_{103}		1.41 d_{222}
1.20 ± 0.03	1.21 ± 0.01		1.21 d_{202}	1.23 d_{110}	1.20 d_{141}
1.07 ± 0.02	1.11 ± 0.01			1.13 d_{006}	1.09 d_{313}

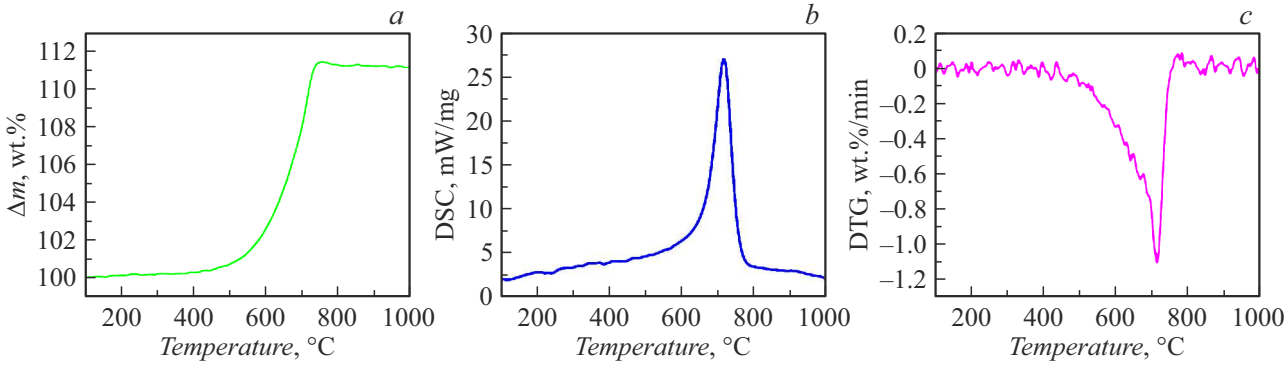

Figure 6. Results of thermogravimetry (*a*), DSC (*b*), differential thermogravimetry (*c*) of the powder of hafnium carbide oxidation (medium — air (100 ml/min), heating rate 10°C/min, temperature interval from 100 to 1000°C).

10°C/min, the gas flow rate was — 150 ml/min. All the studies were under atmospheric pressure. The parameters of the process of thermal conversion of hafnium carbide powder was carried out on the basis of physical quantities (temperature, time and speed of the process) calculated by a graphical method using thermogravimetric, differential thermogravimetric and differential scanning calorimetric curves (TG-, DTG- and DSC-curves) [41].

An analysis of the curves in Fig. 6 allows us to make the following conclusions. Hafnium carbide oxidation starts

at $\sim 400^\circ$C. The DTG data (Fig. 6) make it possible to find that the maximum rate of oxidation of synthesized sample was within the temperature interval $\sim 500-800^\circ$C and is characterized by a single-mode peak. The analysis of Fig. 6, *b* makes it possible to establish that the sample oxidation process occurs with a significant release of energy in the mass gain interval, the maximum heat flux was 27 mW/mg at temperature 718.7°C. Note that the process of oxidation of hafnium carbide, synthesized by the method of thermal action of the direct current arc discharge, proceeds with a significant release of energy in the range of sufficiently high temperatures. The parameters of the hafnium carbide oxidation process proceed with increase in mass (in an oxidizing medium) within 10–12% and subsequent mass stabilization at temperatures above 800°C. Similar oxidation processes are described in the papers of other authors who studied this material obtained by other methods [42]. The results of experimental studies allow us to say that the synthesized powder is characterized by increased oxidation resistance, which may be due to the presence of the oxide film that prevents oxidation processes.

Note that the issues of scaling the presented thermal method for the synthesis of hafnium carbide by increasing the connected power of the reactor simultaneously with the volume increasing of the reaction zone are being worked out at present. The results of these studies will be presented in subsequent papers.

Conclusion

Thus, the paper presents experimental studies on the preparation and characterization of hafnium carbide powder using the thermal effect of atmospheric arc plasma. The series of experiments, in which the current strength (50–220 A) and the duration of thermal exposure (15–75 s) were varied, were carried out on the original electric arc reactor. The technical solutions used made it possible to synthesize a powder containing up to ~ 98 wt.% of the cubic phase of hafnium carbide. It was established that the synthesized hafnium carbide powder is characterized by increased oxidative stability, which is ensured by the presence of an oxide film on the surface of the particles, which increases the oxidation temperature to 500–800°C.

Funding

The research was supported financially by the Russian Science Foundation (grant No .21-79-10030).

Conflict of interest

The authors declare that they have no conflict of interest.

References

[1] C. Young, C. Zhang, A. Loganathan, P. Nautiyal, B. Boesl, A. Agarwal. Ceram. Int., **46** (10), 14625 (2020). DOI: 10.1016/j.ceramint.2020.02.263
[2] J. Cheng, J. Wang, X. Wang, H. Wang. Ceram. Int., **43**, 7159 (2017). DOI: 10.1016/j.ceramint.2017.02.152
[3] R. He, L. Fang, T. Han, G. Yang, G. Ma, J. Liu, X. Chen, L. Xie, L. Liu, Q. Li, Y. Tang, H. Liang, Y. Zou, F. Peng. J. Eur. Ceram. Soc., **42**, 5220 (2022). DOI: 10.1016/j.jeurceramsoc.2022.06.039
[4] X.-L. Qiu, X.-H. Gao, G. Liu. Thin Solid Films, **713**, 1 (2020). DOI: 10.1016/j.tsf.2020.138349
[5] N. Ni, W. Hao, T. Liu, L. Zhou, F. Guo, X. Zhao, P. Xiao. Ceram. Int., **46**, 23840 (2020). DOI: 10.1016/j.ceramint.2020.06.161
[6] D. Demirskyi, O. Vasylkiv, K. Yoshimi. J. Eur. Ceram. Soc., **41**, 7442 (2021). DOI: 10.1016/j.jeurceramsoc.2021.08.038
[7] S. Tian, L. Zhou, Z. Liang, Y. Wang, Y. Yang, X. Qiang, Z. Qian. Ceram. Int., **45**, 19513 (2019). DOI: 10.1016/j.ceramint.2019.06.039
[8] X. Luan, G. Liu, M. Tian, Z. Chen, L. Cheng. Composites Part B, **219**, 1 (2021). DOI: 10.1016/j.compositesb.2021.108888
[9] J. Li, Y. Zhang, Y. Fu, T. Fei, Z. Xi. Ceram. Int., **44**, 13335 (2018). DOI: 10.1016/j.ceramint.2018.04.165
[10] S. Tian, H. Li, Y. Zhang, S. Liu, Y. Fu, Y. Li, X. Qiang. J. Alloys Compd., **580**, 407 (2013). DOI: 10.1016/j.jallcom.2013.04.170
[11] Y. Fu, Y. Zhang, J. Zhang, T. Li, G. Chen. Ceram. Int., **46**, 16142 (2020). DOI: 10.1016/j.ceramint.2020.03.168
[12] N. Patran, N. Al Nasiri, D.D. Jayaseelan, W.E. Lee. Ceram. Int., **42**, 1959 (2016). DOI: 10.1016/j.ceramint.2015.09.166
[13] Q. Wen, Z. Yu, R. Riedel, E. Ionescu. J. Eur. Ceram. Soc., **40**, 3499 (2020). DOI: 10.1016/j.jeurceramsoc.2020.03.067
[14] J.-S. Kim, S.J. Lee, L. Feng, L. Silvestroni, D. Sciti, S.-H. Lee. J. Eur. Ceram. Soc., **40**, 1801 (2020). DOI: 10.1016/j.jeurceramsoc.2019.12.051
[15] Y. Fu, Y. Zhang, J. Zhang, G. Chen, T. Li. Corros. Sci., **185**, 1 (2021). DOI: 10.1016/j.corsci.2021.109443
[16] Y. Fu, Y. Zhang, H. Chen, X. Yin, J. Zhang, J. Sun, Q. Fu. Corros. Sci., **195**, 1 (2022). DOI: 10.1016/j.corsci.2021.110015
[17] Y.-H. Wu, L. Ye, Y.-N. Sun, W.-J. Han, T. Zhao. Chin. J. Polym. Sci., **39**, 659 (2021). DOI: 10.1007/s10118-021-2566-3
[18] Y. Fu, Y. Zhang, X. Yin, L. Han, Q. Fu, H. Li, R. Riedel. J. Mater. Sci. Technol., **129**, 163 (2022). DOI: 10.1016/j.jmst.2022.04.037
[19] A.M. Abdelkader, D.J. Fray. J. Eur. Ceram. Soc., **32**, 4481 (2012). DOI: 10.1016/j.jeurceramsoc.2012.07.010
[20] D. Lu, W. Wang, H. Wang, J. Zhang, Y. Wang, F. Zhang, Z. Fu. Ceram. Int., **42**, 8108 (2016). DOI: 10.1016/j.ceramint.2016.02.012
[21] L. Feng, S.-H. Lee, H. Wang, H.-S. Lee. J. Eur. Ceram. Soc., **35**, 4073 (2015). DOI: 10.1016/j.jeurceramsoc.2015.08.004
[22] B. Matović, B. Babić, D. Bucevac, M. Cebela, V. Maksimović, J. Pantić, M. Miljkovic. Ceram. Int., **39**, 719 (2013). DOI: 10.1016/j.ceramint.2012.06.083
[23] B.B. Bokhonov, D.V. Dudina. Ceram. Int., **43**, 14529 (2017). DOI: 10.1016/j.ceramint.2017.07.164

[24] G.P. Kochanov, I.A. Kovalev, A.I. Ogarkov, S.V. Shevtsov, A.A. Konovalov, A.A. Ashmarin, A.V. Shokod'ko, A.I. Sitnikov, S.S. Strel'nikova, A.S. Chernyavskii, K.A. Solntsev. Inorg. Mater. Appl. Res., **13** (5), 1376 (2022). DOI: 10.1134/S2075113322050203
[25] S. Tian, H. Li, Y. Zhang, S. Zhang, Y. Wang, J. Ren, X. Qiang. J. Cryst. Growth, **384**, 44 (2013). DOI: 10.1016/j.jcrysgro.2013.09.016
[26] A. Pak, A. Ivashutenko, A. Zakharova, Y. Vassilyeva. Surf. Coat. Technol., **387** (2020). DOI: 10.1016/j.surfcoat.2020.1255546
[27] A.Ya. Pak, I.I. Shanenkov, G.Y. Mamontov, A.I. Kokorina. Int. J. Refract. Met. Hard Mater., **93**, 1 (2020). DOI: 10.1016/j.ijrmhm.2020.105343
[28] Y. Su, H. Wei, T. Li, H. Geng, Y. Zhang. Mater. Res. Bull., **50**, 23 (2014). DOI: 10.1016/j.materresbull.2013.10.013
[29] J. Berkmans, M. Jagannatham, R. Reddy, P. Haridoss. Diamond & Relat. Mater., **55**, 12 (2015). DOI: 10.1016/j.diamond.2015.02.004
[30] J. Zhao, L. Wei, Z. Yang, Y. Zhang. Physica E, **44**, 1639 (2012). DOI: 10.1016/j.physe.2012.04.010
[31] J. Zhao, Y. Su, Z. Yang, L. Wei, Y. Wang, Y. Zhang. Carbon, **58**, 92 (2013). DOI: 10.1016/j.carbon.2013.02.036
[32] B. Mahesh, K. Sairam, J.K. Sonber, T.S.R.C. Murthy, G.V.S. Nageswara Rao, T. Srinivasa Rao, J.K. Chakravartty. Int. J. Refract. Met. Hard Mater., **52**, 66 (2015). DOI: 10.1016/j.ijrmhm.2015.04.035
[33] B. Predel. *B-Ba−C-Zr. 1–3* (Springer, 1992)
[34] J. Cheng, J. Wang, X. Wang, H. Wang. Ceram. Int., **43**, 7159 (2017). DOI: 10.1016/j.ceramint.2017.02.152
[35] S. Tian, H. Li, Y. Zhang, J. Ren, X. Qiang, S. Zhang. Appl. Surf. Sci., **305**, 697 (2014). DOI: 10.1016/j.apsusc.2014.03.175
[36] S.K Sarkar., A.D. Miller, J.I. Mueller. J. Am. Ceram. Soc., **55** (12), 628 (1972). DOI: 10.1111/j.1151-2916.1972.tb13457.x
[37] Y.W. Yoo, U.H. Nam, Y. Kim, H.I. Lee, J.K. Park, E. Byon. Appl. Sci. Convergence Technol., **30** (1), 21 (2021). DOI: 10.5757/ASCT.2021.30.1.21
[38] Y. Fu, Y. Zhang, J. Zhang, G. Chen, T. Li. Corros. Sci., **185**, 109443 (2021). DOI: 10.1016/j.corsci.2021.109443
[39] D. Demirskyi, O. Vasylkiv, K. Yoshimi. J. Eur. Ceram. Soc., **41** (15), 7442 (2021). DOI: 10.1016/j.jeurceramsoc.2021.08.038
[40] Y. Jiang, D. Ni, Q. Ding, B. Chen, X. Chen, Y. Kan, S. Dong. RSC Adv., **8** (69), 39284 (2018). DOI: 10.1039/C8RA08123A
[41] A.Y. Pak, G.Y. Mamontov, K.V. Slyusarskiy, K.B. Larionov, S.A. Yankovsky, D.V. Gvozdyakov, V.E. Gubin, R.S. Martynov. Waste Biomass Valorization, **12** (10), 5689 (2021). DOI: 10.1007/s12649-021-01399-w
[42] S. Shimada. Solid State Ionics, **141**, 99 (2001). DOI: 10.1016/S0167-2738(01)00727-5

Translated by I.Mazurov